ACS APPLIED MATERIALS & INTERFACES

Research Article

www.acsami.org

Mechanically Robust, Thermally Stable, Broadband Antireflective, and Superhydrophobic Thin Films on Glass Substrates

Ligang Xu,[†,‡] Zhi Geng,[†,‡] Junhui He,*[,†] and Gang Zhou[†,‡]

[†]Functional Nanomaterials Laboratory and Key Laboratory of Photochemical Conversion and Optoelectronic Materials, Technical Institute of Physics and Chemistry, Chinese Academy of Sciences, Zhongguancundonglu 29, Haidianqu, Beijing 100190, China

[‡]University of Chinese Academy of Sciences, Beijing 100049, China

Supporting Information

ABSTRACT: In this study, we developed a simple and versatile strategy to fabricate hierarchically structured lotus-leaf-like superhydrophobic thin films. The thin films are broadband antireflective, and the average transmittance of coated glass substrates reached greater than 95% in the wavelength range of 530−1340 nm, in contrast to 92.0% for bare glass substrate. The thin film surface shows a static water contact angle of 162° and a sliding angle less than 4°. Moreover, the thin film is thermally stable up to 300 °C, and shows remarkable stability against strong acid, strong alkali, water drop impact, and sand impact abrasion, while retaining its superhydrophobicity. Further, the thin film can pass the 3H pencil hardness test. The current approach may open a new avenue to a variety of practical applications, including windshields, eyeglasses, windows of high rise buildings and solar cells, etc.

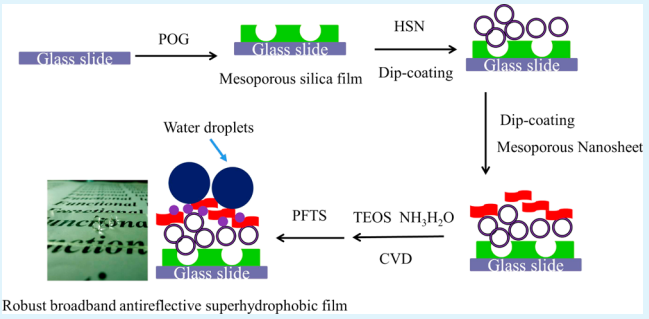

Robust broadband antireflective superhydrophobic film

KEYWORDS: *broadband antireflective, superhydrophobicity, thin films, thermally stable, mechanically robust*

INTRODUCTION

Superhydrophobic thin films, showing a water contact angle (CA) higher than 150° and a sliding angle (SA) lower than 10°, have attracted tremendous attention over the last decade in both academic and industrial areas.[1−5] Their emerging applications include energy conversion,[6] oil−water separation,[7] protection of electronic devices,[8] reducing fluid resistance for aquaculture devices,[9] and avoiding fluid drag in microfluidic devices.[10] Glass substrates having a superhydrophobic thin film are expected to possess those unique functions, and are promising as windows of high rise buildings and protecting covers of solar cells.[11,12]

On the other hand, broadband antireflection has received much attention in the past decades because of its underlying structure−property relationship and wide potential applications.[13−21] For example, antireflective near-infrared optics can be used for night vision, sensors, cancer detection, body scan, and hot-spot detection. Superhydrophobic surfaces with broadband antireflective property could be applied to glass-based substrates such as goggles or windshields and to prevent efficiency degradation of solar cells resulting from pollution accumulation.[22]

Hydrophobicity and transparency are well known to be competitive properties. When roughness increases, hydrophobicity increases, whereas transparency decreases.[2] Therefore, it is currently still a technical challenge to simultaneously achieve both superhydrophobicity and antireflection by an easy and cost-effective method. As a result, the practical application of superhydrophobic coatings has so far been limited on optically transparent materials (such as solar cell glass panels) that require dual-function (superhydrophobicity and antireflection) coatings. Meanwhile, the major issue facing existing techniques for broadband antireflective superhydrophobic thin films is their low ultimate mechanical robustness, but mechanically robust thin films are important and promising for varied applications. Conventional strategies employed to improve film durability typically involve cross-linking the coating layer and/or establishing covalent bonding between the coating and substrate. Zhou et al.[5] reported that a cross-linked elastomeric thin film possessing a nanocomposite structure with a rough and low free-energy surface can endow fabrics with highly durable superhydrophobicity. Alternative approaches to increase thin film durability include introducing self-healing capability to superhydrophobic thin films. For example, Sun et al.[23] reported a self-healing superhydrophobic film that was made of a rigidly flexible porous polymer film with a micro- and nanoscaled hierarchical structure consisting of reacted fluoroalkylsilane in the pores. The film showed excellent self-healing property after oxygen plasma treatment.

Recently, Deng et al.[24] reported a transparent, mechanically robust superhydrophobic film that was made from porous silica capsules. However, the transmittance of the superhydrophobic

Received: December 24, 2013
Accepted: May 21, 2014
Published: May 21, 2014

   dx.doi.org/10.1021/am5016777 | ACS Appl. Mater. Interfaces 2014, 6, 9029−9035

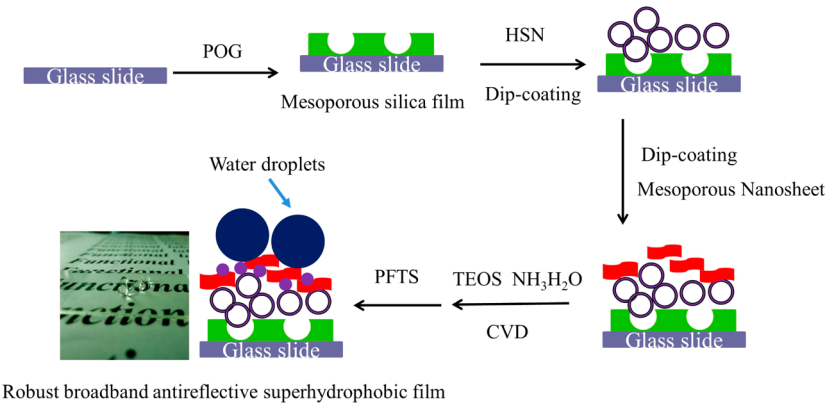

Figure 1. Procedure to prepare the mechanically robust, thermally stable, broadband antireflective, and superhydrophobic thin films on glass substrate.

coating was enhanced only in the short wavelength range (330−410 nm), and was still close to that of the glass substrate. Very recently, our group[25] reported a simple way to build superamphiphobic thin films with broadband antireflective property. Despite the excellent superamphiphobic and antireflective properties, the thin films showed low mechanical robustness. Inspired by the above works,[22,23] we developed in this work a simple and versatile strategy to fabricate mechanically robust, broadband antireflective and superhydrophobic thin films. The thin films have a hierarchical structure. The average transmittance of coated glass substrates reached greater than 95% in the wavelength range of 530−1340 nm, in contrast to 92.0% for bare glass substrate. The thin films were also thermally stable. Meanwhile, the thin films showed remarkable durability against strong acid, strong alkali, water drop impact and sand impact abrasion, while retaining their superhydrophobicity. In addition, the thin films could pass the 3H pencil hardness tests.

EXPERIMENTAL SECTION

Materials. Cetyltrimethylammonium bromide (CTAB, ≥ 99%), aqueous ammonia (25%), absolute ethanol (99.5%), and ethyl ether (≥99.5%) were purchased from Beihua Fine Chemicals. Tetraethyl orthosilicate (TEOS, 99+ %) and 1H,1H,2H,2H-perfluorooctyl--trichlorosilane ($CF_3(CF_2)_5CH_2$ CH_2SiCl_3, PFTS) were obtained from Alfa Aesar. Poly(acrylic acid) (PAA, 30 wt % in water, M_w = 5000) was purchased from Shandong Heli water treatment company. Glass substrates were purchased from Shanghai Xigema Optical and Electric Company. Ultrapure water with a resistivity higher than 18.2 MΩ·cm was used in all experiments and was obtained from a three-stage Millipore Mill-Q Plus 185 purification system (Academic).

Preparation of Hollow Silica Nanoparticles and Mesoporous Silica Nanosheets. Synthesis of 45 nm hollow silica nanoparticles (HSNs): 0.40 g PAA dissolved in 4.5 mL aqueous ammonia was mixed with 90 mL of absolute ethanol, followed by injection of 5 aliquots of TEOS totaling 1.80 mL over a time interval of 50 min under vigorous magnetic stirring at room temperature. After 10 h, 45 nm hollow silica nanoparticles formed.

Synthesis of mesoporous silica nanosheets: 0.5 g of CTAB was dissolved in a mixture composed of 70 mL of water, 0.8 mL of aqueous ammonia, and 20 mL of ethyl ether. After the emulsion system was vigorously stirred for 0.5 h at room temperature, 2.5 mL of TEOS was quickly dripped into the mixture. The resulting mixture was vigorously stirred at room temperature for 4 h, and a white precipitate was obtained, filtered, washed with pure water, and dried in air at 60 °C for 24 h. After calcination of the as-obtained product in air at 550 °C for 5 h to remove its CTAB and other organic components, mesoporous silica nanosheets were eventually obtained.

Thin Film Preparation. Nanoporous silica thin films were deposited on glass substrates by precursor-derived one-step growth. A cleaned glass substrate was immersed in the precursor solution at 60 °C for 20−30 h. Then HSNs nanoparticles and mesoporous silica nanosheets were dip-coated with a HSNs solution (0.25 wt %) and a mesoporous silica nanosheet solution (0.4 wt %), followed by drying at 60 °C for 2 h. Thereafter, the coated glass substrates were placed in an exsiccator together with 2 vessels containing 1 mL of TEOS and 1 mL of ammonia, respectively. CVD of TEOS was performed for 3−24 h at the humid laboratory air (room temperature: 20−30°C). The surfactant template was removed by calcination at 550 °C for 3 h. Then the thin film coated substrate was eventually hardened at 720 °C for 135 s. Finally, the thin films were hydrophobilized by placing 16 μL of PFTS in a Teflon container. In a typical procedure, the autoclave was first put in an oven at 120 °C for 2 h to enable the vapor of PFTS to react with the hydroxyl groups on the film surface. Then the autoclave was opened and placed in an oven at 150 °C for an additional 1.5 h to volatilize unreacted PFTS molecules on the thin film. As a result, the films were coated on both sides of glass substrates.

Characterization. Scanning electron microscopy (SEM) images were obtained on a Hitachi S4800 field-emission scanning electron microscope operated at 5 kV. For transmission electron microscopy (TEM) observations, powder products were dispersed in ethanol by sonication for 10 min, and added onto carbon-coated copper grids. After drying at 60 °C overnight, they were observed on a JEOL JEM-2100F transmission electron microscope at an acceleration voltage of 200 kV. Transmission and reflection spectra in the wavelength range of 200-2000 nm were recorded on a Varian Cary 5000 UV/Vis-NIR spectrophotometer with an integrating sphere attached. Water contact angles (WCAs) of coating surfaces were measured at ambient temperature on a Kino SL200B3 automatic contact angle meter. The angle precision of which is ±0.5°. Water droplets of 1 μL were dropped carefully onto the coating surfaces. The morphology and roughness of coating surfaces were characterized by atomic force microscopy (AFM) on a MM8-SYS scanning probe microscope (Bruker AXR). Pencil hardness was estimated by Elcometer 3086 Motorised Pencil Hardness Tester.

RESULTS AND DISCUSSION

The procedure used to prepare the hierarchically structured broadband antireflective superhydrophobic thin films is schematically presented in Figure 1. A nanoporous silica thin film (see Figure S1a in the Supporting Information) was first deposited on a glass substrate by precursor-derived one-step growth.[26] Then hollow silica nanoparticles (HSNs) of 45 nm (see Figure S1b in the Supporting Information) and mesoporous silica nanosheets (see Figure S1c in the Supporting Information) were sequentially applied onto the nanoporous silica thin film coated glass substrate by dip-coating. The

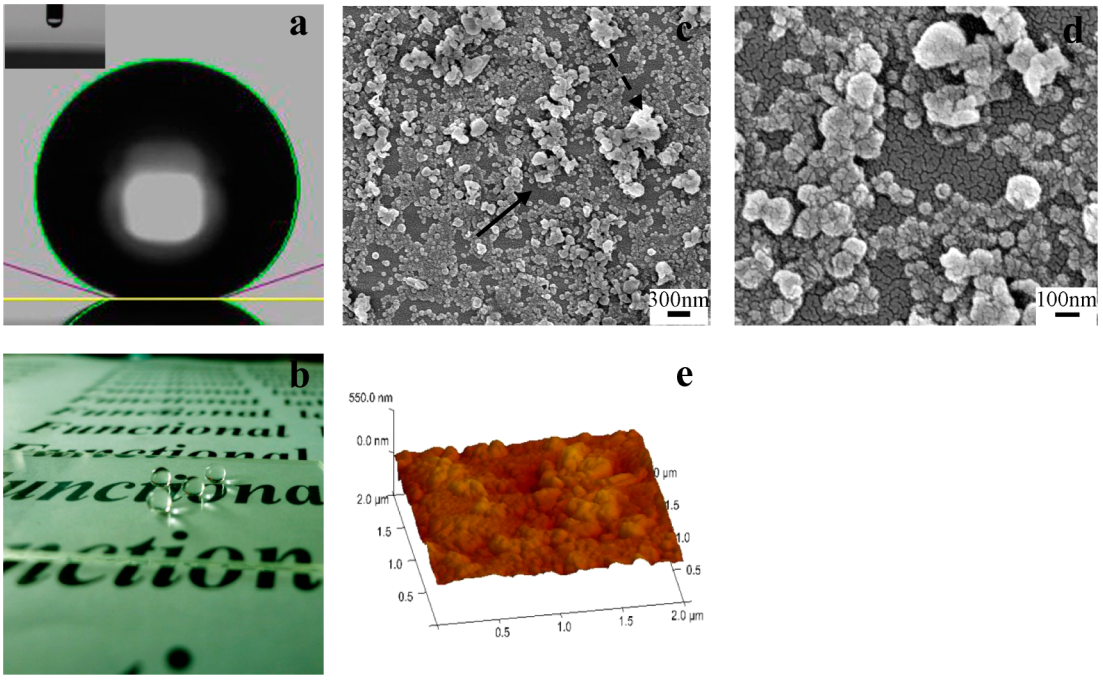

Figure 2. (a) Photograph of a 6 μL water droplet deposited on the superhydrophobic thin film. The thin film surface shows a static water contact angle (WCA) of 162°. (b) Digital photograph of water droplets (10 μL) on the coated glass substrate. (c, d) SEM images of the thin film on glass substrate. (e) 3D-AFM image of the superhydrophobic thin film, scanning area: 2 μm × 2 μm.

mesoporous silica nanosheets and HSNs were chosen to not only lower the refractive index but also increase the surface roughness of thin films. Therefore, multifunctional thin films with both antireflective and superhrophobic properties were fabricated. And such multifunctional thin films could not be fabricated solely by a single-layered nanoporous thin film because of its smooth surface. After the dip-coating, the coated glass substrate was left at room temperature to remove solvent, followed by drying at 60 °C for 2 h. Then chemical vapor deposition (CVD) of tetraethoxysilane (TEOS) in the humid laboratory air in an exsiccator was performed in the presence of ammonia for 3−24 h to enhance the mechanical robustness of thin films (room temperature: 20−30 °C). Then the substrate with the film was eventually hardened at 720 °C for 135 s. The static water contact angle was estimated to 0° (Figure 1a inset picture). After hydrophobization of the film surface by CVD of 1H,1H,2H,2H-perfluorooctyltrichlorosilane (PFTS), the surface exhibited remarkable superhydrophobicity. When a drop of water (6 μL) was placed on the coated glass substrate, a nearly sphere-like water droplet formed with a static contact angle of 162° (Figure 2a). Clearly, the surface energy plays a vital role in the wettability of the coating, and the additional surface modification by PFTS of low surface energy is indispensable for making the surface highly superhydrophobic. The sliding angle was estimated to be below 4° for water droplets of 10 μL. Such spherical droplets were stable and could stay supported on the coated glass substrate for an extended period of time (Figure 2b), showing the stability of superhydrophobicity. SEM images of the coated glass substrate are shown in Figure 2c and d. The coated glass substrate was covered with hollow silica nanoparticles and mesoporous silica nanosheets, which provides roughness on the nanoscale (indicated by arrow) to compliment the microscale roughness (indicated by dashed arrow). The resulting nano/microscale hierarchical roughness on the coated glass substrate is well known to enhance hydrophobicity. Further evidence of the roughness introduced by the thin film is provided by AFM images of the coated glass substrate (Figure 2e). The multifunctional film has a low root-mean-square surface roughness (RMS) of 44.2 nm.[25]

Self-cleaning property was verified by depositing water drops on the superhydrophobic thin film and monitoring the take-up of contaminants (see Figure S2 in the Supporting Information). Self-cleaning is desirable for many applications, such as windows and solar cells. However, both applications require the thin films to be highly transparent or broadband antireflective. In general, transmittance decreases with increasing roughness, especially in the case that the roughness exceeds the wavelength of incident light.[27] The current superhydrophobic thin film has a low surface roughness (RMS = 44.2 nm) from the 3D-AFM image (Figure 2e). Besides, mesopores in the nanosheets and the hollow spheres could also be beneficial to reducing the apparent refractive index of the thin film according to the effective media theory, and are thus beneficial to reducing light reflection and increasing light transmission. The transmittance of coated glass substrate may increase or decrease, depending on the surface roughness and the film thickness and refractive index. According to the UV-VIS-Near IR spectra, the coated glass substrate shows broadband antireflection, and the maximum transmittance reaches as high as 96.5% at the wavelength of 816 nm. The average transmittance of the coated glass substrate is greater than 95.0% in the wavelength range of 530−1340 nm, in contrast to that (92.0%) of bare glass substrate (Figure 3a). The increased transmittance is in line with the strongly reduced reflectance for the corresponding wavelengths. Remarkably enough, the whole spectrum shows reduced reflectance as compared to bare glass substrate, and the minimum reflectance is lowered to essentially 3.6% at 780 nm. According to previous reports,[26] if a glass substrate is only coated by the nanoporous silica thin film, the maximum transmittance can reach as high as

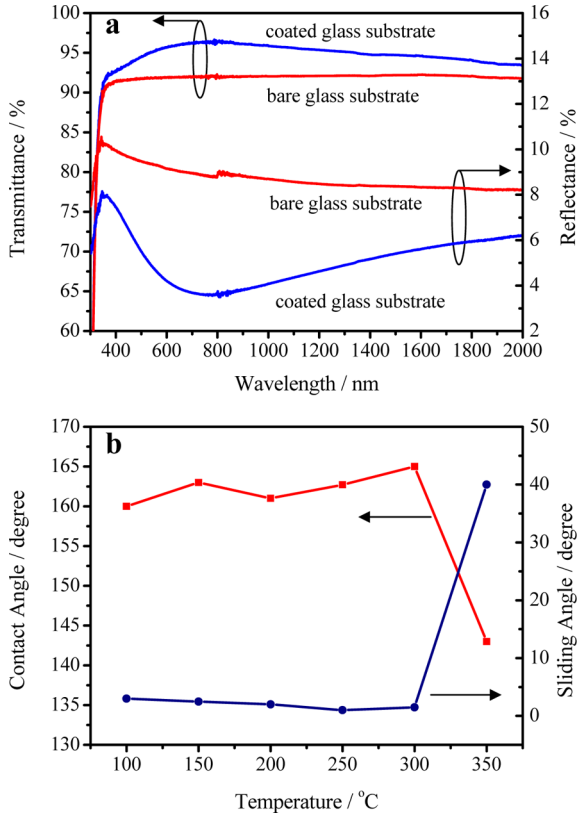

Figure 3. (a) Transmission and reflection spectra of coated glass substrate compared to bare glass substrate. (b) Static water contact angle and sliding angle on the sample annealed for 2 h at varied temperatures. The surface lost its superhydrophobicity after annealing at 350 °C.

99.2 %, i.e., nearly zero reflection at a wavelength of 548 nm, and the thickness of the nanoporous thin film is about 72 nm. The thin film shows a relatively narrow band antireflection. When hollow silica nanoparticles of 45 nm and mesoporous silica nanosheets were sequentially applied onto the nanoporous silica thin film coated glass substrate by dip-coating, the overall film thickness increased, thus exhibiting a red-shift trend of the maximum transmittance wavelength. Meanwhile, the fraction porosity of the nanoporous silica thin film is about 50%,[26] which is higher than that of the HSNs nanoparticles (45 nm) layer (10%) and mesoporous silica nanosheets layer (10%) reported in our previous report.[25] The porosity of the three different layers of the film progressively increases along the incident light, and the pores in the layers may trap and restrain the scattered and reflected light from escaping the coating. As a result, the scattered and reflected light is transmitted through the film. So the thin film showed excellent broad-band antireflective property in the long wavelength range (530 nm to 1340 nm) compared with the nanoporous silica thin film. The high transparency of the coated substrate is also reflected in the good readability of the underneath letters (Figure 2b).

In many applications, surfaces are exposed to elevated temperatures,[28,29] and thus the thermal stability of the superhydrophobic thin film was assessed. The coated substrate was annealed for 2 h at temperatures from 100 to 350 °C, respectively. The static water contact angle (WCA) remained constant up to 300 °C (Figure 3b), documenting the excellent thermal stability of the superhydrophobic thin film. Annealing at even higher temperature could lead to the conversion of the thin film from superhydrophobicity to hydrophobicity (350 °C), even to hydrophilicity. From the previous report,[30] we could know that the desorption of PFTS monolayers occurs at temperatures above 603 K (330 °C). So the WCA of thin film decreased to 142° after annealing at 350 °C for 2 h because of partial desorption of PFTS. After heat treatment at 300 °C for 2 h, the coated glass substrate still showed high broadband antireflection, the maximum transmittance reached as high as 97.0% and the transmittance in the visible spectrum (400−800 nm) even slightly increased, as shown in Figure S3 in the Supporting Information.

Meanwhile, an experiment similar to the damp heat test was also carried out to evaluate the durability of coating. The coated glass substrate was placed at 50°C in 85% RH air for 12 h. It was found that the WCA remained unchanged at 162° after the experiment (Figure 4). Although the transmittance of coated glass substrate slightly decreased, the maximum transmittance was still higher than 96.0% after treatment at 50 °C in 85 RH% air for 12 h.

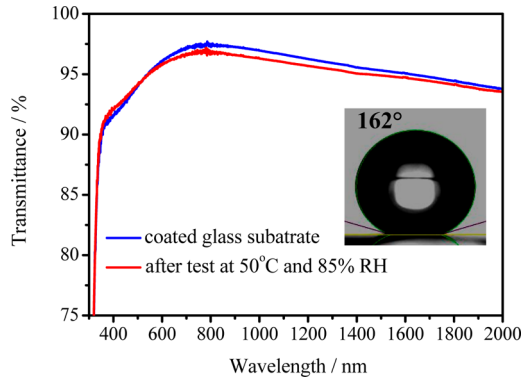

Figure 4. Transmission spectra of coated glass substrate before and after test at 50 °C and 85% RH. The inset is a water contact angle after the test.

Mechanical properties of thin films are a key issue, and must be considered for any possible practical applications. To assess the mechanical properties of the thin film, several complementary tests were carried out. First, water droplets of 22 μL, which could impinge the film surface with a velocity up to v = 3 m/s, were used to test the long-term drop impact stability of the thin film (Figure 5a). After impinging by 5000 water droplets, the WCA was measured to be still above 150°, i.e., 160° (Figure 5b), indicating that the thin film retained its superhydrophobicity. The transmittance of coated glass substrate only decreased slightly in the wavelength range of 400−2000 nm, also pointing to excellent durability of the thin film (Figure 7a).

Superhydrophobic films may contact to strong acid or strong base in daily practical uses. The current film was shown to be very stable when contacting aqueous HCl (pH 1) and aqueous NaOH (pH 14). As shown in Figure 5c, the water contact angle remained unchanged (162 ± 2°) (Figure 4c upper right) and changed to 153 ± 2° (Figure 5c lower right) after contacting to strong acid and strong base for 5 min, respectively (Figure 5c). When the thin film was hydrophobilized by PFTS, most of the mesoporous silica nanosheets and HSNs were modified with fluorosilane. Minor of silica might not be coated with fluorosilane but still with hydroxyl groups (Si−OH). The hydroxyl groups of Si−OH are more philic with base than with

dx.doi.org/10.1021/am5016777 | ACS Appl. Mater. Interfaces 2014, 6, 9029−9035

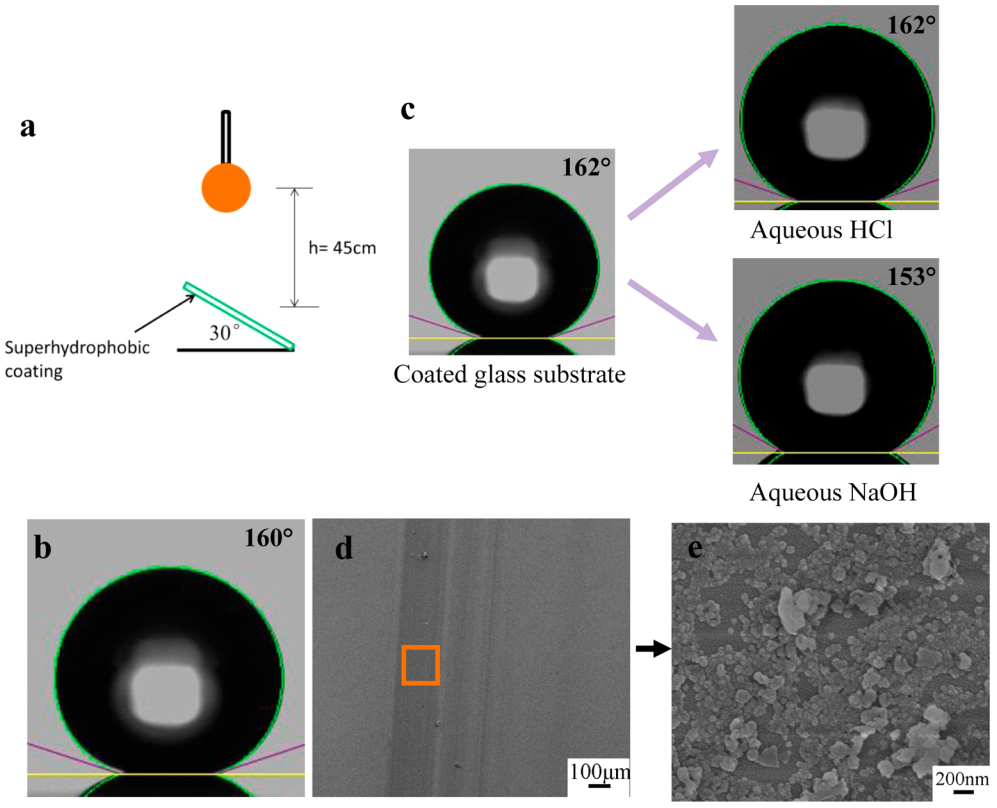

Figure 5. (a) Sketch of the setup for testing the thin film long-term resistance against water droplet impacts. (b) Static water contact angle of the coated glass substrate after impacts of 5000 water droplets. (c) Water droplets (6 μL) on the coated glass substrate before (left) and after contacting either strong acid (upper right) or strong base (lower right) solutions. (d) SEM image of the thin film after scratching with 3H pencil. (e) Magnified image of the scratched area.

acid and water. Thus, the thin film had a lower contact angle with aqueous NaOH than with water and aqueous HCl, but still showed superhydrophobicity. Clearly, the thin film is durable to the attack of strong acid and strong alkali.

A sand impact abrasion test was also performed to investigate the mechanical resistance to sand impact abrasion. Sand grains (20 g, approximately 2.7×10^{13} sand grains, 100 to 350 μm in size) impinged the film surface from a height of 30 cm (Figure 6a), corresponding to an impinging energy of 3.4×10^{-8} J per grain. After sand impact abrasion, the thin film still showed superhydrophobicity with a water contact angle of 160° (Figure 6b). SEM images (Figure 6c, d) show the surface of coated glass substrate before and after a sand impact abrasion test. It is noted that the densities of the HSNs and mesoporous silica nanosheets decreased after sand impact abrasion. This density decrease may account for the slight decrease in WCA. However, the remaining HSNs and silica nanosheets still showed an overall nano/microscale morphology, which made the surface keep its superhydrophobicity. From Figure 7b, it is also found that the coated glass substrate still showed broadband antireflection. Although the transmittance of coated glass substrate slightly decreased after sand impact abrasion test, its maximum transmittance was still higher than 96.0%, pointing to excellent mechanical robustness of the thin film.

Meanwhile a pencil hardness test was performed to evaluate the mechanical robustness of the thin film. If a thin film is attached to the substrate surface by van der Waals interactions, it usually could not stand for 1B pencil hardness tests. SEM images (Figure 5d and e) show that most of the HSNs and nanosheets were still attached on the coated glass substrate

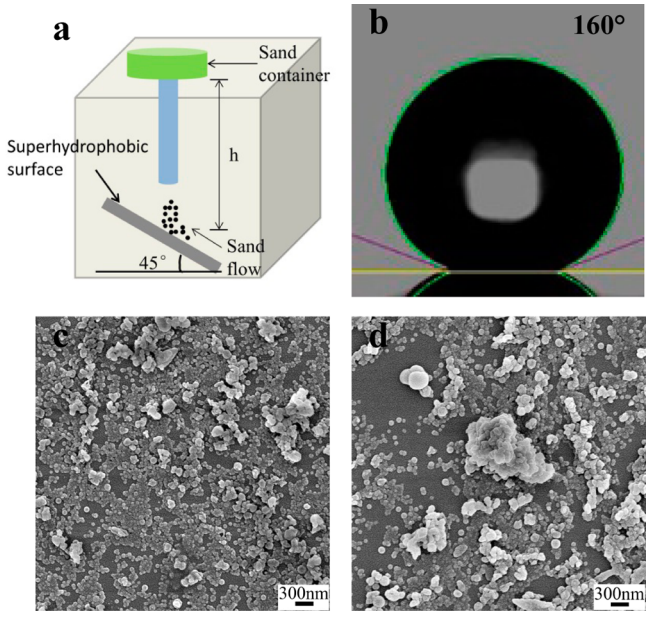

Figure 6. Mechanical robustness quantified by sand impact abrasion. (a) Schematic drawing of the set-up for sand impact abrasion test, (b) water droplet deposited on the thin film after 20 g sand impact abrasion from a 30 cm height. The 100–350 μm sized grains have a velocity of 8.7 km/h just before impingement. SEM images of the thin film (c) before and (d) after a sand impact abrasion test.

after a 3H pencil hardness test, indicating that the current superhydrophobic and antireflective film could stand for 3H

dx.doi.org/10.1021/am5016777 | ACS Appl. Mater. Interfaces 2014, 6, 9029–9035

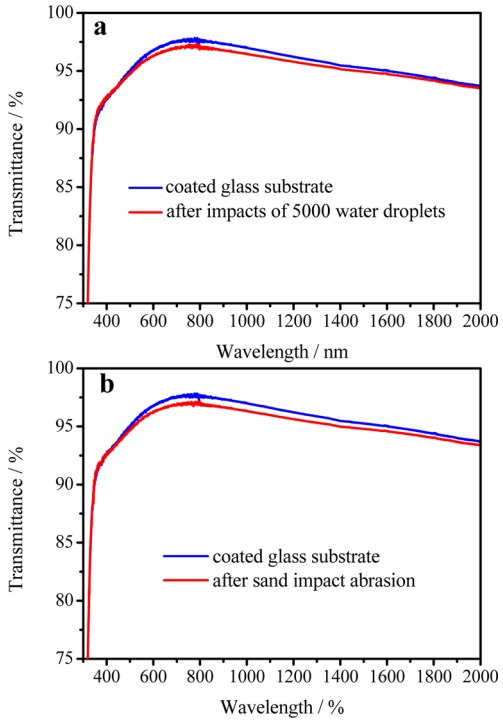

Figure 7. (a) Transmission spectra of coated glass substrate before and after impacts of 5000 water droplets. (b) Transmission spectra of coated glass substrate before and after sand impact abrasion.

pencil hardness test. After a 4H pencil hardness test (see Figure S4a, b in the Supporting Information), however, the HSNs and silica nanosheets were almost removed from the glass substrate but still had the thin film fabricated by precursor-derived one-step growth. So the overall thin film could not pass 4H pencil hardness test.

CONCLUSION

In summary, we developed a simple and versatile strategy to fabricate hierarchically structured lotus-leaf-like superhydrophobic thin films. The thin films are broadband antireflective, and the average transmittance of coated glass substrates reached greater than 95% in the wavelength range of 530−1340 nm, in contrast to 92.0% for bare glass substrate. The thin film surface shows a static water contact angle of 162° and a sliding angle less than 4°. Moreover, the thin film is thermally stable up to 300 °C, and also shows remarkable stability against strong acid, strong alkali, water drop impact, and sand impact abrasion, while retaining its superhydrophobicity. Further, the thin film can pass 3H pencil hardness test. To the best of our knowledge, this is the first example that simultaneously shows excellent broadband antireflection, superhydrophobicity, high mechanical robustness, and excellent thermal stability. If the mechanical robustness of the multifunctional films could be further enhanced, they are promising in a variety of practical applications, including windshields, eyeglasses, windows of high rise buildings and solar cells, etc.

ASSOCIATED CONTENT

Supporting Information

TEM images of nanoporous silica thin film (a), hollow silica nanospheres (b), and mesoporous silica nanosheets (c), respectively (Figure S1), Sand polluted superhydrophobic surface (a) before and (b) after water drops took up the contaminants encountered on its way (Figure S2), transmission spectra of coated glass substrate before and after heat treatment at 300 °C for 2 h (Figure S3), SEM images of the thin film after scratching with 4H pencil (Figure S4), UV−Vis−NIR transmission spectra of coated glass substrate after varied periods of time of TEOS CVD, and the static water contact angles of the thin film after varied periods of time of TEOS CVD (Figure S5). This material is available free of charge via the Internet at http://pubs.acs.org.

AUTHOR INFORMATION

Corresponding Author

*E-mail: jhhe@mail.ipc.ac.cn. Fax: +86 10 82543535.

Notes

The authors declare no competing financial interest.

ACKNOWLEDGMENTS

This work was supported by the National High Technology Research and Development Program ("863" Program) of China (Grant 2011AA050525), the Knowledge Innovation Program of the Chinese Academy of Sciences (CAS) (Grants KGCX2-YW-370 and KGCX2-EW-304-2), the National Natural Science Foundation of China (Grant 21271177), and Key Laboratory of Space Energy Conversion Technology, TIPC, CAS.

REFERENCES

(1) Tuteja, A.; Choi, W.; Ma, M.; Mabry, J. M.; Mazzella, S. A.; Rutledge, G. C.; McKinley, G. H.; Cohen, R. E. Designing Superoleophobic Surfaces. *Science* **2007**, *318*, 1618−1622.

(2) Nakajima, A.; Fujishima, A.; Hashimoto, K.; Watanabe, T. Preparation of Transparent Superhydrophobic Boehmite and Silica Films by Sublimation of Aluminum Acetylacetonate. *Adv. Mater.* **1999**, *11*, 1365−1368.

(3) Ma, M.; Gupta, M.; Li, Z.; Zhai, L.; Gleason, K. K.; Cohen, R. E.; Rubner, M. F.; Rutledge, G. C. Decorated Electrospun Fibers Exhibiting Superhydrophobicity. *Adv. Mater.* **2007**, *19*, 255−259.

(4) Xu, L.; He, J. Fabrication of Highly Transparent Superhydrophobic Coatings from Hollow Silica Nanoparticles. *Langmuir* **2012**, *28*, 7512−7518.

(5) Zhou, H.; Wang, H.; Niu, H.; Gestos, A.; Wang, X.; Lin, T. Fluoroalkyl Silane Modified Silicone Rubber/Nanoparticle Composite: A Super Durable, Robust Superhydrophobic Fabric Coating. *Adv. Mater.* **2012**, *24*, 2409−2412.

(6) Nosonovsky, M.; Bhushan, B. Energy transitions in Superhydrophobicity: low Adhesion, easy Flow and Bouncing. *J. Phys.: Condens. Matter* **2008**, *20*, 395005.

(7) Pan, Q.; Wang, M.; Wang, H. Separating small amount of water and hydrophobic solvents by novel superhydrophobic copper meshes. *Appl. Surf. Sci.* **2008**, *254*, 6002−6006.

(8) Mishchenko, L.; Hatton, B.; Bahadur, V.; Taylor, J. A.; Krupenkin, T.; Aizenberg, J. Design of Ice-free Nanostructured Surfaces Based on Repulsion of Impacting Water Droplets. *ACS Nano* **2010**, *4*, 7699−7707.

(9) Shi, F.; Niu, J.; Liu, J.; Liu, F.; Wang, Z.; Feng, X. Q.; Zhang, X. Towards Understanding Why a Superhydrophobic Coating Is Needed by Water Striders. *Adv. Mater.* **2007**, *19*, 2257−2261.

(10) Ou, J.; Rothstein, J. P. Direct Velocity measurements of the flow past Drag-Reducing Ultrahydrophobic Surfaces. *Phys. Fluids* **2005**, *17*, 103606.

(11) Li, X.; Du, X.; He, J. Self-Cleaning Antireflective Coatings Assembled from Peculiar Mesoporous Silica Nanoparticles. *Langmuir* **2010**, *26*, 13528−13534.

(12) Xu, L.; Gao, L.; He, J. Fabrication of visible/near-IR Antireflective and Superhydrophobic Coatings from Hydrophobically modified Hollow Silica Nanoparticles and Poly(methyl methacrylate). *RSC Adv.* **2012**, *2*, 12764−12769.

(13) Liu, L.-Q.; Wang, X.-L.; Jing, M.; Zhang, S.-G.; Zhang, G.-Y.; Dou, S.-X.; Wang, G. Broadband and Omnidirectional, Nearly zero reflective Photovoltaic Glass. *Adv. Mater.* **2012**, *24*, 6318−6322.
(14) Huang, Y.-F.; Chattopadhyay, S.; Jen, Y.-J.; Peng, C.-Y.; Liu, T.-A.; Hsu, Y.-K.; Pan, C.-L.; Lo, H.-C.; Hsu, C.-H.; Chang, Y.-H.; Lee, C.-S.; Chen, K.-H.; Chen, L.-C. Improved Broadband and Quasi-omnidirectional Anti-reflection properties with Biomimetic Silicon nanostructures. *Nat. Nanotechnol.* **2007**, *2*, 770−774.
(15) Du, Y.; Luna, L. E.; Tan, W. S.; Rubner, M. F.; Cohen, R. E. Hollow Silica Nanoparticles in UV−Visible Antireflection Coatings for Poly(methyl methacrylate) Substrates. *ACS Nano* **2010**, *4*, 4308−4316.
(16) Li, X.; He, J. In situ Assembly of Raspberry- and Mulberry-like Silica Nanospheres toward Antireflective and Antifogging Coatings. *ACS Appl. Mater. Interfaces* **2012**, *4*, 2204−2211.
(17) Liu, X.; Du, X.; He, J. Hierarchically structured porous Films of Silica Hollow Spheres via Layer-by-Layer assembly and their Superhydrophilic and Antifogging properties. *ChemPhysChem* **2008**, *9*, 305−309.
(18) Xu, L.; He, J. Antifogging and Antireflection Coatings Fabricated by Integrating Solid and Mesoporous Silica Nanoparticles without Any Post-Treatments. *ACS Appl. Mater. Interfaces* **2012**, *4*, 3293−3299.
(19) Yao, L.; He, J. Multifunctional Surfaces with Outstanding Mechanical Stability on Glass Substrates by Simple H2SiF6-Based Vapor Etching. *Langmuir* **2013**, *29*, 3089−3096.
(20) Xu, L.; He, J.; Yao, L. Fabrication of Mechanically Robust Films with high Transmittance and durable Superhydrophilicity by Precursor-derived One-step Growth and post-treatment. *J. Mater. Chem. A* **2014**, *2*, 402−409.
(21) Moghal, J.; Kobler, J.; Sauer, J.; Best, J.; Gardener, M.; Watt, A. A. R.; Wakefield, G. High-Performance, Single-Layer Antireflective Optical Coatings Comprising Mesoporous Silica Nanoparticles. *ACS Appl. Mater. Interfaces* **2011**, *4*, 854−859.
(22) Zhu, J.; Hsu, C.-M.; Yu, Z.; Fan, S.; Cui, Y. Nanodome Solar Cells with Efficient Light Management and Self-Cleaning. *Nano Lett.* **2009**, *10*, 1979−1984.
(23) Li, Y.; Li, L.; Sun, J. Bioinspired Self-Healing Superhydrophobic Coatings. *Angew. Chem.* **2010**, *122*, 6265−6269.
(24) Deng, X.; Mammen, L.; Zhao, Y.; Lellig, P.; Müllen, K.; Li, C.; Butt, H.-J.; Vollmer, D. Transparent, Thermally Stable and Mechanically Robust Superhydrophobic Surfaces Made from Porous Silica Capsules. *Adv. Mater.* **2011**, *23*, 2962−2965.
(25) Geng, Z.; He, J.; Xu, L.; Yao, L. Rational design and elaborate construction of Surface Nano-structures toward highly Antireflective Superamphiphobic Coatings. *J. Mater. Chem. A* **2013**, *1*, 8721−8724.
(26) Xu, L.; He, J. A Novel Precursor-derived One-step Growth approach to fabrication of highly Antireflective, Mechanically Robust and Self-healing Nanoporous Silica thin Films. *J. Mater. Chem. C* **2013**, *1*, 4655−4662.
(27) Li, Y.; Zhang, J.; Zhu, S.; Dong, H.; Jia, F.; Wang, Z.; Sun, Z.; Zhang, L.; Li, Y.; Li, H.; Xu, W.; Yang, B. Biomimetic Surfaces for High-Performance Optics. *Adv. Mater.* **2009**, *21*, 4731−4734.
(28) Deng, X.; Mammen, L.; Butt, H.-J.; Vollmer, D. Candle Soot as a Template for a Transparent Robust Superamphiphobic Coating. *Science* **2012**, *335*, 67−70.
(29) Janssen, R. A. J.; Hummelen, J. C.; Sariciftci, N. S. Sariciftci. Polymer−Fullerene Bulk Heterojunction Solar Cells. *MRS Bull.* **2005**, *30*, 33−36.
(30) Khatri, O. P.; Devaprakasam, D.; Biswas, S. K. Frictional Responses of Octadecyltrichlorosilane (OTS) and 1H, 1H, 2H, 2H-Perfluorooctyltrichlorosilane (FOTS) Monolayers Self-assembled on Aluminium over Six Orders of Contact Length Scale. *Tribol Lett.* **2005**, *20*, 235−246.